

PREDICTION MODELS FOR LOAD CARRYING CAPACITY OF RC WALL THROUGH NEURAL NETWORK

Shaheera Sharib¹, Naveed Ahmad¹, Vagelis Plevris² and Afaq Ahmad¹

¹ Civil Engineering Department, University of Engineering & Technology Taxila, Pakistan
e-mail: shaheera.sharib@students.uettaxila.edu.pk,
naveed.ahmad@uettaxila.edu.pk, afaq.ahmad@uettaxila.edu.pk

² Department of Civil and Architectural Engineering, Qatar University
P.O. Box: 2713, Doha, Qatar
e-mail: vplevris@qu.edu.qa

Abstract

This study is focused on the development of prediction models for the determination of the load carrying capacity of reinforced concrete walls using Artificial Neural Networks (ANNs). A database of 95 samples is used for the RC Wall, based on available experimental studies, including various critical parameters, such as the length of web portion of the wall (L_w), thickness of wall boundary member (b_w), effective depth of wall (d), height of wall (H), shear span ratio (a_v/d), vertical steel ratio (ρ_v), horizontal steel ratio (ρ_h), yield strength of vertical and horizontal steel (f_y), compressive strength of concrete (f_c), and the ultimate load carrying capacity (V_{exp}). Depending on the combination of the input parameters, 4 different ANN models are trained by using a customized code in Matlab. Several error metrics have been used for the evaluation of the performance of the various ANN models. The comparative study exhibited that the predictions of the ANN model are closer to the experimental values as compared to their counterpart physical models, i.e., the compressive force path (CFP) and the current design codes, ACI and Eurocode 2.

Keywords: Neural Network, ANN, CFP, ACI, EC2, RC Wall.

1 INTRODUCTION

Extensive research work has been conducted on studying the behavior of the RCC shear walls during the recent years [1]. These walls provide higher strength and rigidity to the buildings, resist large horizontal seismic forces, and reduce lateral sway and damage to other structural members [2]. The shear walls of the building should be arranged symmetrically in plane to reduce the adverse effects of distortion of the building. They can be placed symmetrically along one or, optimally, both directions of the plane. When the shear walls are located on the outer periphery of the building, they are most effective as they can provide more torsional stiffness to the building, increasing the building's capacity in resisting twist [2].

Internal forces, such as axial loads, shear forces and bending moments are developed in RC shear walls when the building is subjected to loading. Based on the aspect ratio of the shear wall (shear span length divided by the height of the wall), shear walls are usually divided into thin (high-rise) and low (low-rise) ones [3]. A ductile failure mechanism overshadowed by bending deformation near the bottom of the wall is more likely in thin, high-rise walls. On the other hand, because of their geometry, low-rise walls often undergo a failure mechanism controlled by shear. Figure 1 (a)-(d) shows some typical failure modes of a shear wall.

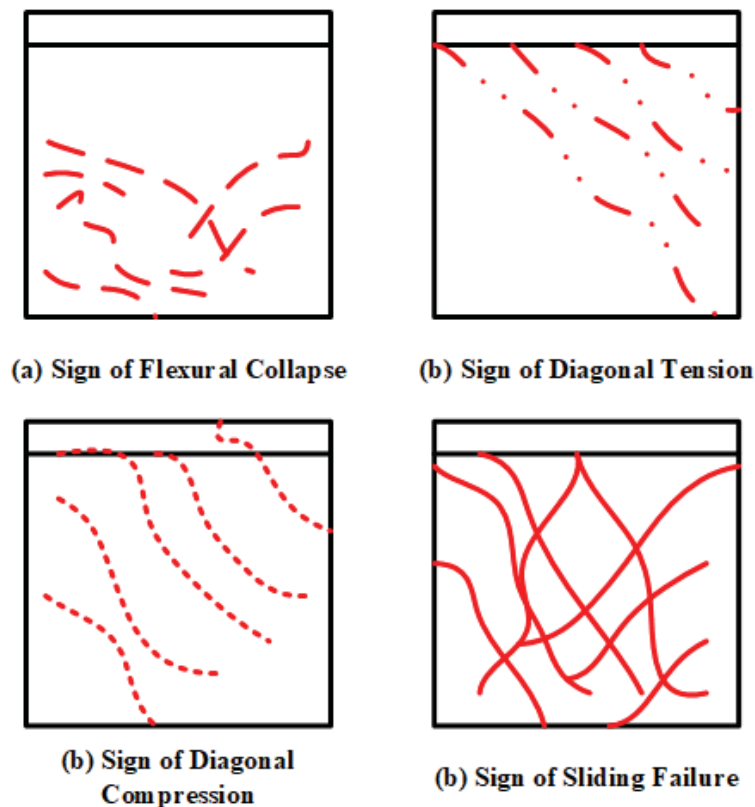


Figure 1: Typical failure modes of a shear wall.

ACI-318 [4] indicates that if the aspect ratio of the wall is greater than 3.0, the wall is considered thin (generally controlled by bending), while if its aspect ratio is less than 1.5, it is considered a low-rise wall or low wall (generally controlled by shear). If the aspect ratio of the walls is between 1.5 and 3.0, the resulting behavior will be affected by both shear and bending. According to Eurocode 2 (EC2) [5] relatively tall and well-designed shear walls (with aspect ratio greater than 3) generally exhibit ductile flexural failure because of their higher shear

strength. Figure 1 (a) shows the development of flexural failure, possibly due to concrete crushing or longitudinal bars fracture in the plastic zone of the hinge. It has been observed that flexural failure is uncommon in squat shear walls, especially the ones having aspect ratio less than one as shown in Figure 1 (b) to (d). When the horizontal shear reinforcement of the wall is insufficient resulting in the development of one or more diagonal cracks, diagonal stress failure is likely to occur, as shown in Figure 1 (b). When the wall has a sufficient horizontal shear reinforcement, a diagonal compression failure will occur, as illustrated in Figure 1 (c), where concrete collapses under oblique (diagonal) pressure and cracks are widely distributed. Compared to rectangular section shear walls, walls with boundary elements (the end thicker part of the walls, as illustrated in Figure 1) have a greater chance of oblique compression failure because they can exhibit higher flexural strength, increasing the requirement for web shear [4]. Compression failure or diagonal failure can be reduced by providing sufficient horizontal shear reinforcement and limiting the nominal shear stresses. The occurrence of slip shear failure may be due to (i) large cracks produced at the base of the wall; and (ii) concrete crushing and buckling of steel bars along the narrow band of the wall base, as shown in Figure 1 (d), after the bending steel is significantly deformed.

The theory through which the loads are transferred within the RC wall, at the ultimate limit state (ULS), is based on “Truss Analogy” models in most current design codes [4, 5]. The relevant equations of design codes, such as EC2 [5] and ACI [4] are essentially empirical in nature, usually based on data fitting processes. However, the results obtained from these design codes appear to be significantly different with respect to their experimental counterparts. One of the possible reasons for this is the different nature of the analysis formulas used in the available codes. The aim of the current study is to analyze the load carrying capacity of reinforced concrete walls using ANN, i.e. a non-conventional problem-solving technique and compare it with current design codes, i.e., conventional models. For this purpose, a database of 95 samples of RC Wall (WAL) under lateral loading is used, with detailed information collected from previous studies, including details of the critical parameters. Four different ANN models are examined, and their results are compared to each other based on several error metrics. The comparative study exhibited that the predictions of the ANN model are closer to the experimental values as compared to their counterpart physical models, i.e.; compressive force path (CFP) [6] and also the current design codes (CDCs), i.e. ACI and EC2.

2 RCC SHEAR WALL DATABASE

For this work, a database was prepared consisting of 95 samples, including the details of the critical parameters, as described in Table 1, i.e. length of web portion of the wall (L_w), *thickness of wall boundary member* (b_w), effective depth of wall (d), height of wall (H), shear span ratio (a_v/d), vertical steel ratio (ρ_v), horizontal steel ratio (ρ_h), yield strength of vertical and horizontal steel (f_y), compressive strength of concrete (f_c), and ultimate load carrying capacity (V_{exp}) for the RC Wall, as illustrated in Figure 2 and Table 1. In addition to the minimum and maximum values of these parameters, the mean, standard deviation and coefficient of variation is also reported in the table. Figure 3 shows the correlation value R [7, 8] of the critical parameters against the experimental value V_{exp} .

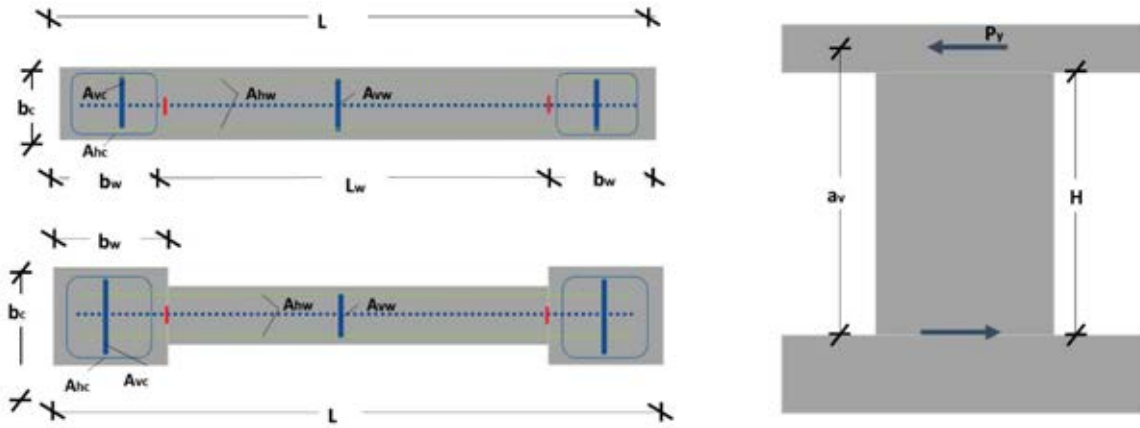


Figure 2: Plan and cross-section of RC shear wall used in the analysis.

Description	Unit	Min	Max	Mean	St.Dev	COV
Length of web portion of the wall (L_w)	mm	650	1700	961.68	302.33	0.31
Thickness of wall boundary member (b_w)	mm	65	130	95.58	18.25	0.19
Effective depth of wall (d)	mm	520	1360	771.5	240.92	0.31
Height of wall (H),	mm	610	4570	1567.61	746.78	0.48
Shear span ratio (a_v/d),		0.86	3.04	2.19	0.62	0.28
Vertical steel ratio (ρ_v)= $A_{vw}/b_w \cdot s_v$		0.35	3.33	2.98	1.57	1.02
Horizontal steel ratio (ρ_h)= $A_{hw}/b_w \cdot s_h$	MPa	0.11	1.57	0.62	0.32	0.52
Yield strength of vertical and horiz. steel (f_y)	MPa	375	622	247	506.59	63.63
Compressive strength of concrete (f_c)	MPa	20.1	53.8	33.69	7.05	0.21
Ultimate load carrying capacity (V_{exp})	kN	65	980	280.69	221.53	0.79

Table 1: Statistical properties of the database for RC Wall.

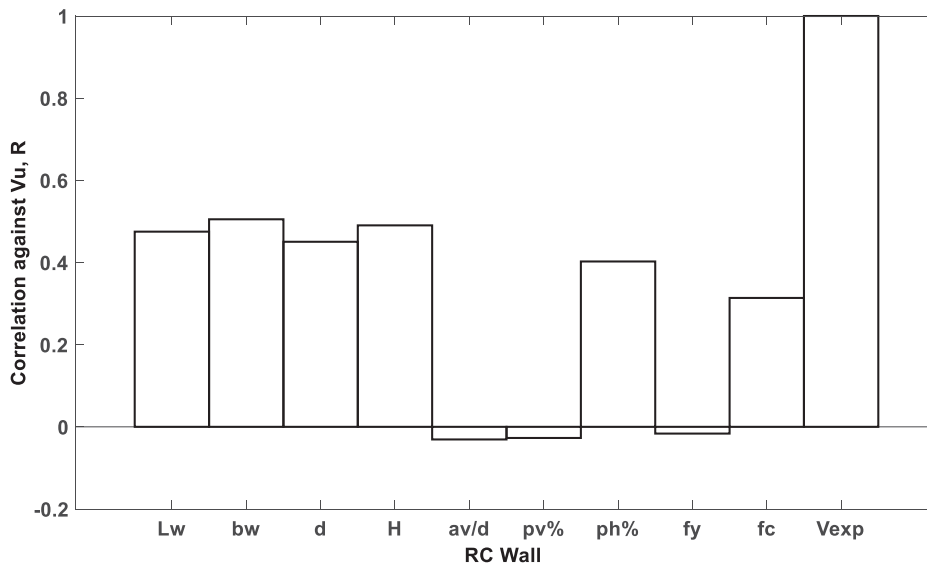


Figure 3: Variation of correlation factor R with respect to the critical parameters of RC Shear Wall.

3 MODELLING OF ARTIFICIAL NEURAL NETWORKS (ANN)

Neural networks simulate the human and animal nervous systems and biological neural networks in the brain [9]. These networks are used to evaluate functions based on a large number of input data parameters. ANNs can learn, classify, summarize, and predict the values of variables because they can keep the information presented to them during the training process in their memory, and because of their adaptability. They are composed of several connected layers, each of which contains a complex interconnected neuron system. There is a link between every two neurons in continuous layers, with a specific weight. Then the prediction of the neuron is multiplied by these weights. In this latter process, the prediction of the neuron is passed through the link and added to the bias as shown in Figure 4 (a). The Multilayer Feedforward ANN (MLFNN) is considered to be suitable for handling these types of problems. MLFNN has an input layer, an output layer, and one or more hidden layers. In this study, we specifically use Back-Propagation Neural Networks (BPNNs) [10]. BPNN is a feedforward multi-layer network with a standard structure. That is, neurons are not interconnected within a layer, but are connected to all neurons in the previous and subsequent layers. For this type of ANN, the output value is cross-validated with the target response to get the error value. During many training cycles to reduce error values, different techniques are used, changing the weight of each link [11, 12]. In this case, it can be said that the network has learned the function of a particular goal. As the name of the algorithm suggests, errors are propagated back from the output node to the input node. The architecture of the ANN is defined by the number of hidden layers and the number of neurons in each layer, as illustrated in Figure 4.

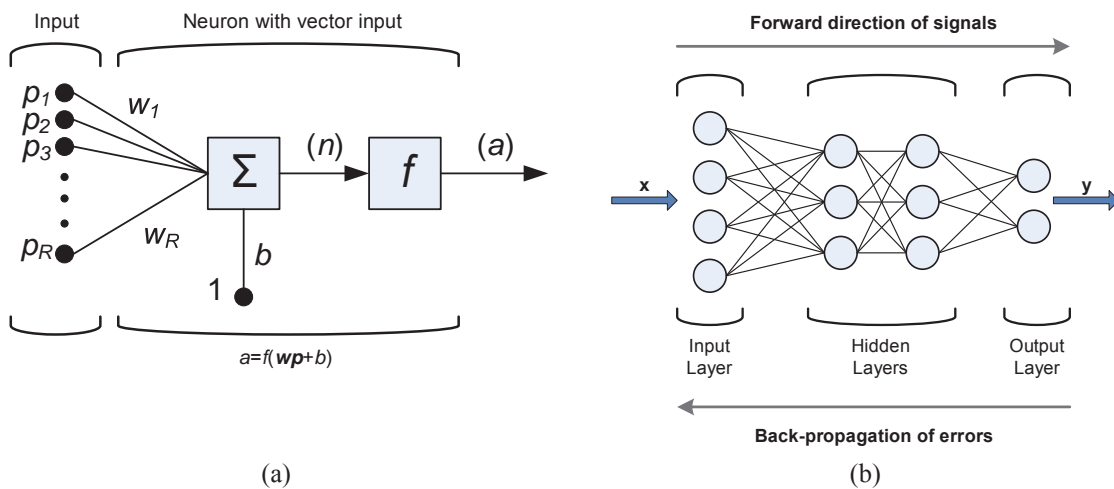


Figure 4: (a) Mathematical function of neuron, and (b) Typical layout of back propagation Neural Network.

As shown in Figure 4, BPNN is made up of numerous layers, each layer comprising a complex system of interrelated ‘neurons’. There are certain weights and links between the neurons and the weights are multiplied by values generated by the neurons. Later on, the values created by the neuron are moved through the link and then biased as shown in Figure 4, where a single node (neuron) in a hidden layer is represented with one R -element input vector. Eq. (1) represents this summation as a predefined function as

$$a = f\left(\sum w_i p_i + b\right) \quad (1)$$

where, b is the bias value, a is the neuron output, p_i are the input values and w_i are the weight coefficients. The above equation can also be written in matrix form as

$$a = f(\mathbf{w}\mathbf{p} + b) \quad (2)$$

Where \mathbf{w} is a row vector ($1 \times R$) and \mathbf{p} is a column vector ($R \times 1$), so that their matrix product, $\mathbf{w}\mathbf{p}$ is a scalar. The values for the input process of the next layer of neurons is produced by the output of the activation function. The final value of the weight is obtained during the learning process based on the available data after a random initial weight is first assigned. The error generated through the process can be calculated by Eq. (3):

$$E(\mathbf{w}) = \frac{1}{2} \sum_i (T_i - O_i)^2 \quad (3)$$

where T_i are the target values (defined in the database) and O_i are the output values predicted by the ANN. The details of the critical parameters, i.e., length of web portion of the wall (L_w), thickness of wall boundary member (b_w), effective depth of wall (d), height of wall (H), shear span ratio (a_v/d), vertical steel ratio (ρ_v), horizontal steel ratio (ρ_h), yield strength of vertical and horizontal steel (f_y), compressive strength of concrete (f_c), and ultimate load carrying capacity (V_{exp}) for the RC Wall are presented in Table 1. The specific parameters used for the different ANN models are presented in Table 2.

ANN Name	Set of Input Parameters used	Output Parameter
WAL-1	$L_w, b_w, d, H, a_v/d, \rho_v, \rho_h, f_y, f_c$	
WAL-2	$L_w, b_w, H, a_v/d, f_c, M_f/f_c b_w d^2$	V_{exp}
WAL-3	$b_w/d, a_v/d, \rho_v f_y / \rho_h, f_c / f_y$	
WAL-4	$b_w/d, a_v/d, M_f/f_c b_w d^2, f_c / f_y$	

Table 2: The four ANNs used and the sets of the input parameters used for every case.

ANNs works well on normalized input/output data. The problem of low learning rate could be solved using the process described in [11, 12]. In the current study, all the parameters related to RCC shear wall were normalized using the expression of Eq. (4). All parameters used are unitless.

$$X = \frac{\Delta X}{\Delta x} x + \left(X_{\max} - \frac{\Delta X}{\Delta x} x_{\max} \right) \quad (4)$$

In the above formula, x is the actual value, X is the normalized value, Δx is the difference between the maximum and the minimum x values, x_{\max} is the maximum value for variable x , X_{\max} is the new required maximum value for X , ΔX is the new required difference between the maximum and the minimum X values.

In this study, we use $X_{\max}=0.7$ and $\Delta X=0.9$ in order to obtain normalized values in the range of [0.1, 0.9]. To study the precision of the generated models, the proposed ANN models need to be calibrated with obtained experimental results. For the calibration of the ANN model, the multi-layer free forward back-propagation (MLFFBP) process is used along with testing results process as proposed by the authors [11-17].

V_u	Unit	MIN	MAX	DIFF	AVG	SD	COV
V_{exp} (target value)	kN	83	977	894	269.83	176.43	0.65
WAL-1 prediction	kN	93	950	857	262.03	179.36	0.68
WAL-2 prediction	kN	96	978	882	267.45	173.14	0.65
WAL-3 prediction	kN	92	753	661	292.81	182.03	0.62
WAL-4 prediction	kN	109	817	708	291.38	177.84	0.61

Table 3: Performance of the different ANN models for RC Wall.

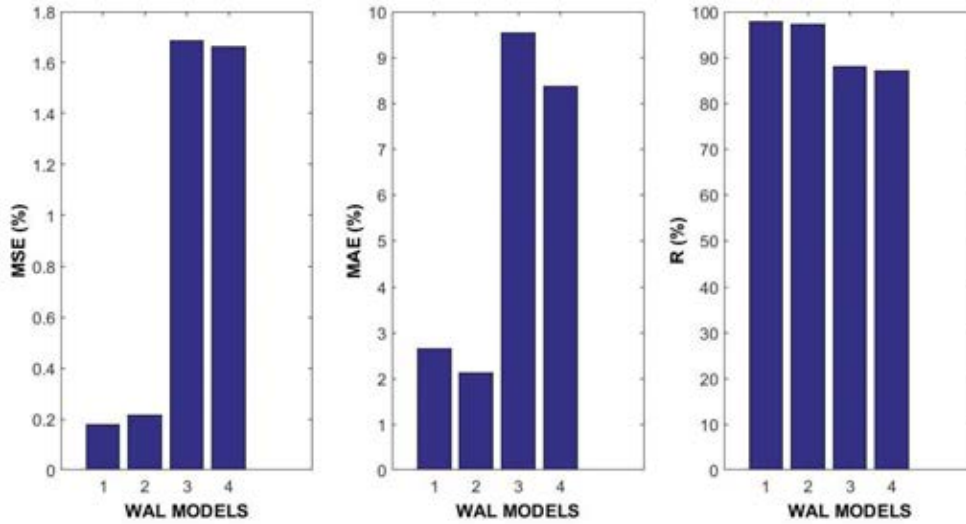


Figure 5: Performance of the various ANN models for the case of RCC Shear Wall.

Table 3 presents the performance of the four different ANN models used for strength (target values) prediction. Minimum values, maximum values, their difference, average, median, standard deviation, and coefficient of variation have been presented for different models. The Pearson correlation coefficient R , mean square error MSE , and mean absolute error MAE are calculated using Eqs. (5), (6) and (7), respectively. In case the ANN outputs O_i match the targets T_i perfectly, then R will have a value of 1, while the MSE and MAE values will be zero [11, 12].

$$R = \frac{\sum_{i=1}^n [(T_i - \bar{T})(O_i - \bar{O})]}{\sqrt{\sum_{i=1}^n (T_i - \bar{T})^2 \cdot \sum_{i=1}^n (O_i - \bar{O})^2}} \quad (5)$$

$$MSE = \frac{\sum_{i=1}^n (T_i - O_i)^2}{n} \quad (6)$$

$$MAE = \frac{\sum_{i=1}^n |T_i - O_i|}{n} \quad (7)$$

In the above equations, T_i and O_i values have been established experimentally and by using ANN models, respectively. Here, n represents the number of data points, while \bar{T} and \bar{O} represent the average values for the experimental and the predicted values, respectively. The values for MSE , MAE and R as obtained from different ANN models proposed for RC wall are presented in Figure 6. In this study, WAL-2 is the model corresponding to highest R value (98%) and lowest MSE (0.22%) and MAE (2.05%) values, as shown in Figure 5. Figure 6 shows the predictions of the different ANN models in comparison to the experimental (target) values.

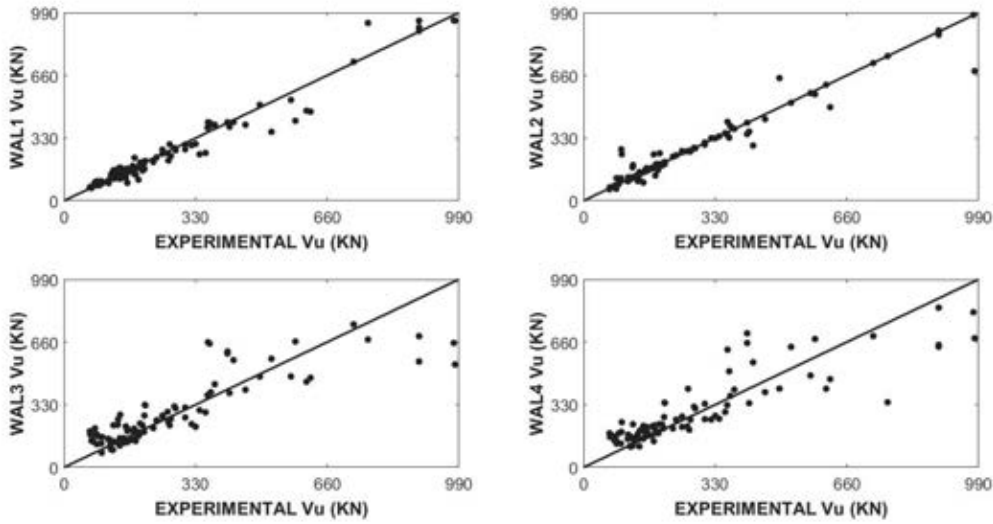


Figure 6: Predictions of the four examined ANN models for RC wall.

4 COMPARATIVE STUDY

This section discusses a comparative study between the proposed ANN model, the CFP method [6] the CDCs, i.e. the ACI and EC models [4, 5]. The corresponding results of the different methods vs the experimental values are presented in Figure 7. The results show that the ANN and CFP are closer to the EXP as compared to the CDCs.

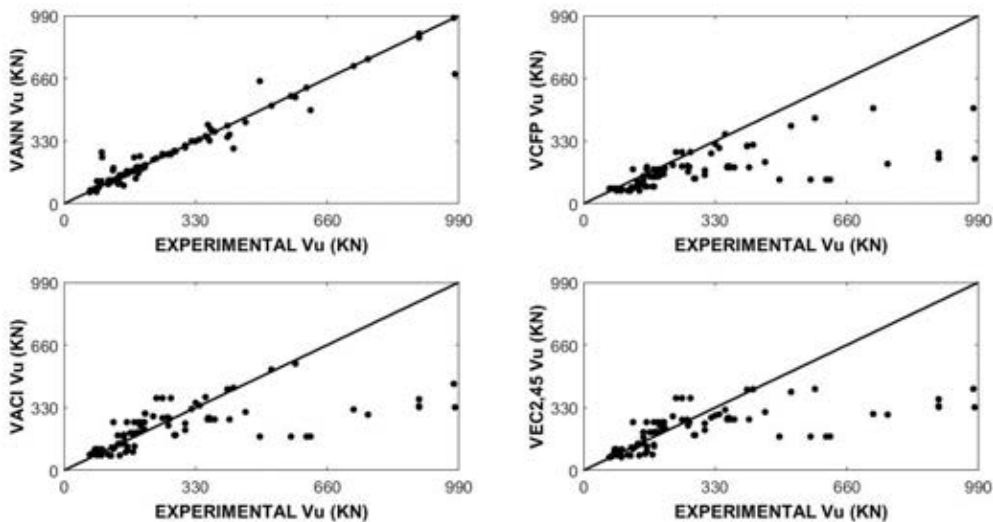


Figure 7: Comparative analysis of ANN predictions for RC wall with physical models.

Figure 8 presents the Gaussian distribution of the ratios, where the ANN (expressed as V_{exp}/V_{ANN}) exhibits the least standard deviation of 1.05.

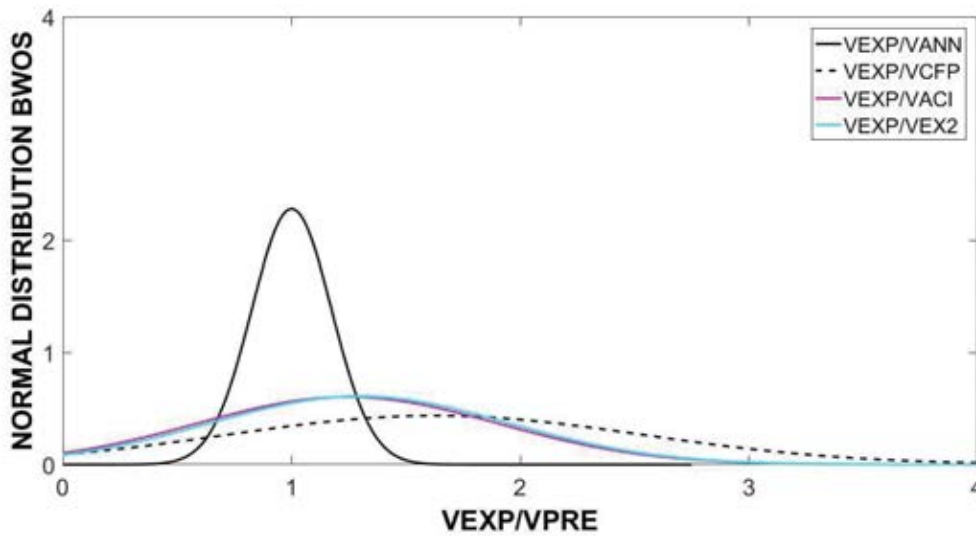


Figure 8: Normal distribution curves for the various prediction models.

Figure 9 shows the overestimate and underestimate values for ULS, where a value of 1 for V_{exp}/V_{pre} signifies the best prediction. We see that 90% of the results of the non-conventional models i.e.; ANN and CFP lie in the accurate range (near 1) i.e. [0.755, 1.255], while the CDCs results, i.e. ACI and EC2, have more samples in the other ranges. The CDC models underestimate the value of V , in comparison to the ANN models and the CFP method.

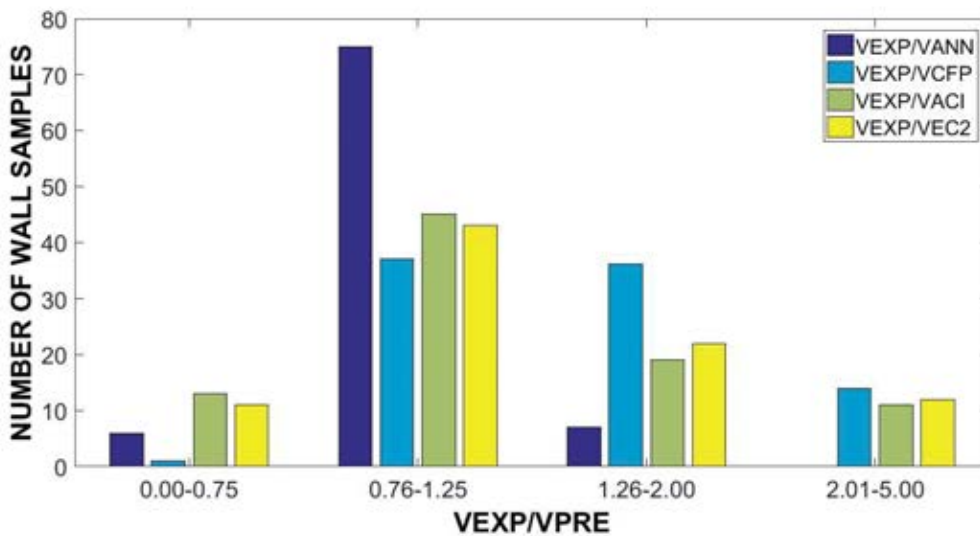


Figure 9: Ratios of V_{exp}/V_{pred} for RC wall.

5 CONCLUSIONS

The research work illustrated the capability of the ANN modelling for RC wall with fixed support at the bottom under the lateral loading, while considering the critical parameters, i.e. length of web portion of the wall (L_w), thickness of wall boundary member (b_w), effective depth of wall (d), height of wall (H), shear span ratio (a_v/d), vertical steel ratio (ρ_v), horizontal steel

ratio (ρ_h), yield strength of vertical and horizontal steel (f_y), compressive strength of concrete (f_c), and ultimate load carrying capacity (V_{exp}) for the RC Wall. Four ANN models were examined, and the second model (WAL-2 ANN) showed the best performance in terms of the error metrics values (MSE , MAE and R values). The comparative study exhibited that the prediction of the non-conventional model, i.e., the ANN model is closer to the provided experimental values in comparison to the other physical models, i.e., CFP and CDCs. This result is in accordance with the results of other researchers working on different databases. Unlike the conventional methodology, soft computing techniques like ANN models have the capability to predict the response of the RC member with simple or complex geometry under different loading conditions. Once the ANNs are trained on the provided database, they can provide an accurate prediction without pertaining to material behavior and the mechanism underlying structural response of RC at ULS.

REFERENCES

1. Harne, V.R., *Comparative study of strength of RC shear wall at different location on Multi-storied residential building*. International Journal of Civil Engineering Research, 2014. **5**(4): p. 391-400.
2. Chandurkar, P. and D.P. Pajgade, *Seismic analysis of RCC building with and without shear wall*. International Journal of Modern Engineering Research (IJMER), 2013. **3**(3): p. 1805-1810.
3. Mohammadi-Doostdar, H., *Behaviour and design of earthquake resistant low-rise shear walls*. 1994: University of Ottawa (Canada).
4. ACI, *Building Code Requirements for Structural Concrete (ACI 318-14) and Commentary*, in *aci-318-14*. 2014: American Concrete Institute 38800 Country Club Drive Farmington Hills, MI 48331. p. 1-471.
5. EC2, *Eurocode 2: Design Of Concrete Structures - Part 1-1: General Rules And Rules For Buildings*, in *EN 1992-1-1*. 2004: Management Centre: Avenue Marnix 17, B-1000 Brussels.
6. Kotsovos, M.D., *Compressive Force-Path Method*. Springer Cham Heidelberg New York Dordrecht London: Springer.
7. Giordano, F., M.L. Rocca, and C. Perna, *Input Variable Selection in Neural Network Models*. Communications in Statistics-Theory and Methods, 2014. **43**(4): p. 735-750.
8. LeCun, Y., et al., *Efficient Backprop*. 1998: Red Bank, NJ 07701-703, USA. p. 1-44.
9. Basheer, I.A. and M. Hajmeer, *Artificial Neural Networks: Fundamentals, Computing, Design, And Application*. Journal of Microbiol Methods, 2000. **43**(1): p. 3-31.
10. Rojas, R., *The Backpropagation Algorithm*, in *Neural Networks*. 1996, Springer: Verlag, Berlin, 1996. p. 151-184.
11. Ahmad, A., N.D. Lagaros, and D.M. Cotsovos, *Neural Network-Based Prediction: The Case of Reinforced Concrete Members under Simple and Complex Loading*. Applied Sciences, 2021. **11**(11): p. 4975.
12. Ahmad, A., V. Plevris, and Q.-u.-Z. Khan, *Prediction of Properties of FRP-Confined Concrete Cylinders Based on Artificial Neural Networks*. Crystals, 2020. **10**(9): p. 811.
13. Ahmad, A., et al., *Assessing the accuracy of RC design code predictions through the use of artificial neural networks*. International Journal of Advanced Structural Engineering, 2018. **10**(4): p. 349-365.
14. Ahmad, A. and A. Raza, *Reliability Analysis of Strength Models for CFRP-Confined Concrete Cylinders*. Composite Structures, 2020: p. 112312.

15. Asteris, P.G. and V. Plevris, *Anisotropic masonry failure criterion using artificial neural networks*. Neural Computing Applications, 2017. **28**(8): p. 2207-2229.
16. Plevris, V. and P.G. Asteris, *Modeling of masonry failure surface under biaxial compressive stress using Neural Networks*. Construction Building Materials, 2014. **55**: p. 447-461.
17. Raza, A. and A. Ahmad, *Reliability analysis of proposed capacity equation for predicting the behavior of steel-tube concrete columns confined with CFRP sheets*. Computers Concrete, 2020. **25**(5): p. 383-400.